RSC Advances

PAPER

View Article Online
View Journal | View Issue



Cite this: *RSC Adv.*, 2020, **10**, 6503

# Multi-factor study of the effects of a trace amount of water vapor on low concentration $CO_2$ capture by 5A zeolite particles†

Hui Wang,[a] Ying Yin,[b] Junqiang Bai*[a] and Shifeng Wang[c]

Water vapor is ubiquitous and affects the performance of an adsorbent. In this work, a grand-canonical Monte Carlo method (GCMC) combining with dispersion-corrected density functional theory (DC-DFT) calculation is adopted to investigate the effect of a trace amount of water vapor on low concentration $CO_2$ capture in 5A zeolite particles. The force field parameters for the interactions among $CO_2$, water, and 5A zeolite are obtained *via* DC-DFT calculations. The effects of the charges of water molecules on the $CO_2$ and $N_2$ adsorption amounts and the selectivity of the $CO_2/(N_2 + O_2)$ gas mixture under different trace amounts of water vapor ranging from 0.05 ppm to 5 ppm are studied. The results show that the presence of the water vapor in 5A zeolite particles increases or decreases the $CO_2$ adsorption amount, which is strongly determined by the trace amount of water. Specifically, when the water vapor concentration is less than 0.1 ppm, the $CO_2$ adsorption amount is increased by 0.7–53.4%, whereas when the water vapor concentration is greater than 0.3 ppm, the amount of adsorbed $CO_2$ decreases, with the reduction proportional to the amount of trace water. However, the $N_2$ adsorption amount and the selectivity of the $CO_2/(N_2 + O_2)$ gas mixture decrease with an increasing amount of trace water. This indicates that the electrostatic interactions induced by the water molecules are the dominant factor influencing the $CO_2$ and $N_2$ adsorption amount and the selectivity of the $CO_2/(N_2 + O_2)$ gas mixture. Therefore, to achieve the desired adsorption performance, a trace amount of water vapor (<0.1 ppm) is recommended for $CO_2$ adsorption, whereas low trace amounts of water vapor (<0.1 ppm) are also recommended for the selectivity of the $CO_2/(N_2 + O_2)$ gas mixture in the 5A zeolite particle.

Received 12th October 2019
Accepted 31st January 2020

DOI: 10.1039/c9ra08334k

rsc.li/rsc-advances



## 1. Introduction

Adsorption bed systems have attracted much attention in recent years due to their important applications in space stations where they are used to remove the carbon dioxide ($CO_2$) produced by the astronauts and maintain a sustainable living environment.[1] The adsorption bed system is a gas purification device within which a large number of nanoporous adsorbent particles are filled. Currently, the widely used adsorbent particles in the adsorption bed system of the space station are 5A zeolite particles because of their robust structure at high temperatures and high adsorption for low concentrations of $CO_2$.[2] Under the operational conditions, 5A zeolite particles are able to adsorb the low concentration $CO_2$ produced by the astronauts and equipment. However, in addition to the $CO_2$, a low concentration of water vapor also exists in the space station atmosphere.[3] The presence of water vapor affects the capability of 5A zeolite particles to capture the low concentration of $CO_2$, which further changes the overall performance of the adsorption bed system for the gas adsorption and separation.[4] Therefore, it is necessary to investigate the effect of water vapor on the gas adsorption and separation performance of the 5A zeolite particles in the space station.

The effects of water vapor on the gas adsorption and separation by zeolite particles are usually studied by experimental measurements. For example, Kraus *et al.*[5] investigated the competitive adsorption of toluene at the relative humidity of 64% on the various zeolites such as the 3A, 4A, and 5A zeolites. They found that the competitive adsorption of toluene and water vapor is related to the Si/Al ratio, zeolite type, binder type and crystallinity. However, the influence of water vapor on the toluene adsorption in the zeolite was not elucidated. Bal'zhinimaev *et al.*[6] experimentally studied toluene adsorption in the pure silica zeolites in the absence and presence of a water vapor with a volume fraction of 1.38%. The amount of adsorbed toluene was found to be similar for various silica zeolites because of the effect of the strong binding of water vapor on the adsorption sites. Zito *et al.*[7] studied the permeation of the $CH_4$,

[a]School of Aeronautics, Northwestern Polytechnical University, Xi'an, Shaanxi 710072, China. E-mail: junqiang@nwpu.edu.cn

[b]MOE Key Laboratory of Thermo-Fluid Science and Engineering, School of Energy and Power Engineering, Xi'an Jiaotong University, Xi'an, Shaanxi 710049, China

[c]School of Engineering, Newcastle University, Newcastle, NE1 7RU, UK

† Electronic supplementary information (ESI) available. See DOI: 10.1039/c9ra08334k

$H_2$, and CO gases in the 4A zeolite in the presence of a water vapor with a volume fraction of 2.2% in the temperature range of 300–700 K, and found that the presence of water vapor clearly reduces the amounts of the adsorbed $CH_4$, $H_2$, and CO gases. However, the studies of the effect of water vapor on the gas adsorption capacity in zeolites are restricted by the capabilities and accuracy of the experimental tool used to study this effect. Moreover, the mechanism of the competitive adsorption of the water vapor and other gases that is important for the practical application of an adsorption material cannot be clearly elucidated by experimental measurements, particularly for three-component gases.

Molecular simulations such as grand canonical Monte Carlo (GCMC) simulations can overcome the above drawbacks and provide an alternative method for elucidating the mechanism of the competitive adsorption of different gases in adsorbents.[8–11] For example, Jing *et al.*[12] used the GCMC method to simulate the adsorption process of a $CO_2/N_2$ gas mixture in the MCM-41 zeolite. They found that the adsorption heats for the $CO_2$ and $N_2$ gases decrease with increasing adsorption amount. Then, Kim *et al.*[13] reported that 15% hydration of the solvation cage can improve the diffusion capability of sodium in the zeolite. In another study, Jeong *et al.*[14] examined $CO_2$ adsorption in hundreds of silica zeolites at different humidities ranging from 1.04% to 3.14%. It was found that the presence of water vapor can reduce the $CO_2$ adsorption amount in some silica zeolites compared to the dry $CO_2$ adsorption in zeolite, which was interpreted as due to the separation of the $CO_2/H_2O$ binding sites. Subsequently, Ahunbay *et al.*[15] used GCMC to study water vapor adsorption in the Na–ZSM-5 zeolite, and found that at a low water vapor coverage, two water molecules were located in the vicinity of the strongly hydrophilic Al sites. Joos *et al.*[16] studied the adsorption behavior of the $H_2O/CO_2$ (1 : 99) gas mixture in the 13X zeolite. They reported that water vapor can reduce the amount of adsorbed $CO_2$ by an order of magnitude. Recently, Wang *et al.*[17] used the GCMC method to investigate the adsorption behavior of a $CO_2/N_2/O_2$ gas mixture in 5A zeolite in the space station. Although they have considered the adsorption of low concentration $CO_2$ in 5A zeolite, the effect of water vapor on the low concentration $CO_2$ capture in the 5A zeolite particles was ignored.

The studies mentioned in the above survey of the literature focus on the high concentration gas adsorption properties or dry gas adsorption in zeolites. However, removing the low concentration $CO_2$ in the space station is rarely studied at the molecular level. The mechanism of water vapor on the low concentration $CO_2$ capture is not well-understood. A four-bed molecular sieve apparatus is widely used to remove the low-concentration $CO_2$ in space stations. The adsorption bed filled with 5A zeolite particles is the key component of the four-bed molecular sieve apparatus. Although most of the water vapor is removed by the water vapor adsorption system, a trace amount of water vapor with a concentration ranging from 0.05 to 5 ppm can enter the 5A zeolite particle adsorption bed. Thus, the effect of a trace amount of water vapor on the low concentration $CO_2$ capture should be considered. Owing to the lower amount of adsorbed $O_2$ in the 5A zeolite compared to that of $N_2$, the adsorption of $O_2$ can be ignored at the atmospheric pressure.[18,19] Thus, only three adsorbed gases ($N_2$, $CO_2$, and water) are involved. The effects of the water vapor concentration on the adsorption of $CO_2$ and $N_2$, as well as the low concentration $CO_2$ capture in the 5A zeolite particles should be thoroughly investigated.

To this end, the grand-canonical Monte Carlo method (GCMC) combining with a dispersion-corrected density functional theory (DC-DFT) calculation is adopted in this work to study the effects of the trace amount of water vapor on the $CO_2$ and $N_2$ adsorption and the selectivity of the $CO_2/(N_2 + O_2)$ ($N_2/O_2/CO_2$; 0.78 : 0.21966 : 0.00034) gas mixture at the different water vapor pressures and concentrations. The effects of the partial charges of the water molecule on the amounts of $CO_2$ adsorption only and $N_2$ adsorption only, and on the selectivity of the $CO_2/(N_2 + O_2)$ gas mixture are also examined.

## 2. Molecular simulation method

Pressure and temperature should be treated as input parameters in the GCMC method. In the present work, the temperature of the space station is 288 K, and the pressure varies from 0 to 120 kPa. The unit cell of the 5A zeolite ($S_n = 1$) is chosen because the same periodic unit cells exist in the 5A zeolite particle,[20,21] as shown in Fig. 1. The molecular formula of 5A zeolite is written as $Ca_{34}Na_{28}Al_{96}Si_{96}O_{384}$. Periodic boundary conditions are adopted for the simulation box with a rigid structure.

The sodium and calcium cations move in the 5A zeolite according to the method described in ref. 22 and 23. A rigid linear triatomic molecule with a bond length of 0.116 nm is used to represent the $CO_2$ molecule. The potential energy $U_{ij}$ includes the Coulomb potential ($U_{Eq}$) and Lennard-Jones (L-J) potential ($U_{LJ}$) energy terms and is given by

$$U_{ij} = U_{Eq} + U_{LJ} = \frac{q_i q_j}{4\pi\varepsilon_0 r_{ij}} + 4\varepsilon_{ij}\left[\left(\frac{\sigma_{ij}}{r_{ij}}\right)^{12} - \left(\frac{\sigma_{ij}}{r_{ij}}\right)^{6}\right], \quad (1)$$

where $q_i$ and $q_j$ are the partial charges of atoms i and j, respectively, $\varepsilon_0$ is the dielectric constant ($8.85 \times 10^{-12}$ F m$^{-1}$), $r_{ij}$ is the distance between atoms i and j, $\sigma_{ij}$ is the L-J diameter, and

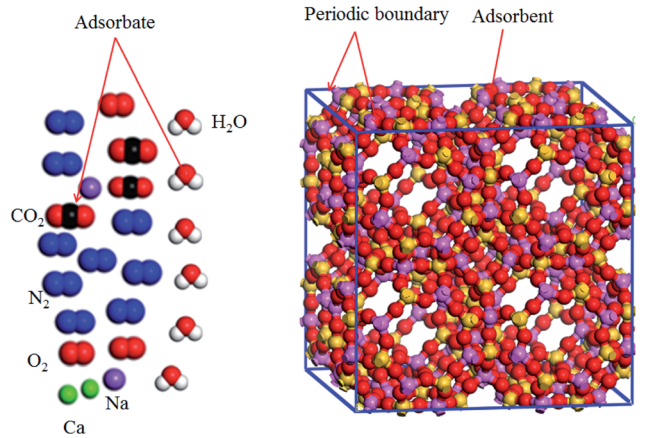


Fig. 1 Unit cell of 5A zeolite used for the GCMC model calculations.

$\varepsilon_{ij}$ is the L-J depth. The Ewald summation technique is adopted for the evaluation of the electrostatic interactions. The cutoff radius for the L-J interactions is set to 1.24 nm, and the Lorentz–Berthelot mixing rules are used for all L-J cross-interaction parameters. Furthermore, the $N_2$ molecule is treated as three atoms with one pseudoatom.[24] The water molecules are treated using the four-point transferable interaction potential (TIP4P) model.[25] All of the parameters of the L-J potential between the 5A zeolite and $CO_2$, $N_2$, and water are obtained by periodic dispersion-corrected density functional theory (DFT) calculations using VASP 5.4.[26,27] The values of the atomic partial charges are obtained using the density-derived electrostatic and chemical charges for the atoms of the 5A zeolite. The details of the calculation procedures are similar to those described in ref. 28–30. The values of the L-J potential parameters and atomic partial charges for $CO_2$, $N_2$ and water are shown in Tables S1(a) and (b) (ESI).†

The random removal, displacement, and insertion are repeated during the GCMC simulation. The acceptance probabilities for the random insertion, random deletion, and movement are given in eqn (2)–(4).

$$p_{m\to n}^{*+} = \min\left\{1,\ \frac{fV}{kTN_n}\ \exp\left[-\frac{1}{kT}(U_n - U_m - \mu)\right]\right\} > \xi \quad (2)$$

$$p_{m\to n}^{*-} = \min\left\{1,\ \frac{kTN_m}{fV}\ \exp\left[-\frac{1}{kT}(U_n - U_m + \mu)\right]\right\} > \xi \quad (3)$$

$$p_{m\to n}^{*} = \min\left\{1,\ \exp\left[-\frac{1}{kT}(U_n - U_m)\right]\right\} > \xi \quad (4)$$

where $\xi$ is a random number between 0 and 1, $V$ is the volume, $U_n$ and $U_m$ are the potential energies of configurations n and m, respectively, and $N_n$ and $N_m$ are the numbers of adsorbent molecules of configurations n and m, respectively. The pressure ($p$) is obtained from the fugacity ($f$) by solving the Peng–Robinson equation, as shown in eqn (5). $\mu$ is the chemical potential as defined in eqn (6):

$$f = p\ \exp\left\{Z - 1 - \ln\left(Z - \frac{bp}{RT}\right) - \frac{a}{2\sqrt{2}bRT}\ \ln\left\{\left[Z + \left(1+\sqrt{2}\right)\frac{bp}{RT}\right]\Big/\left[Z + \left(1-\sqrt{2}\right)\frac{bp}{RT}\right]\right\}\right\} \quad (5)$$

$$\mu = -kT\ \ln\left[\frac{V}{(N_m+1)\Lambda^3}\right] - kT\ \ln\langle\exp[-(U_n - U_m)/(kT)]\rangle_{N_m} \quad (6)$$

where $Z$ is the compressibility factor, $a$ and $b$ are coefficients, $\Lambda$ is the de Broglie thermal wavelength, and $\langle\ \rangle$ is the ensemble average. The values of these parameters are shown in Table S2 (ESI).† The first $1 \times 10^7$ steps are repeated to obtain identical chemical potentials for the adsorbed and bulk phases. Then, another $1 \times 10^7$ steps are used to obtain the converged potential energy and number of adsorbates. Then, the excess adsorption amount ($N$) can be calculated as

$$N = 1000\left(\frac{N_{am}M_i}{S_n} - \rho V_{fv}N_A\right)\Big/(M_s M_i) \quad (7)$$

where $M_s$, $M_i$, $V_{fv}$, $N_{am}$, and $N_A$ are the number of the crystal unit cells, relative molecular mass of the adsorbate, free volume of the crystal unit cell, final number of the adsorbate molecules, and Avogadro's constant, respectively. $\rho$ is the bulk density given by:

$$\rho = \frac{pM_i}{ZRT} \quad (8)$$

The adsorption heat ($Q$) is given by

$$Q = RT - \frac{\langle U_{ff}N_{am}\rangle - \langle U_{ff}\rangle\langle N_{am}\rangle}{\langle N_{am}^2\rangle - \langle N_{am}\rangle\langle N_{am}\rangle} - \frac{\langle U_{fs}N_{am}\rangle - \langle U_{fs}\rangle\langle N_{am}\rangle}{\langle N_{am}^2\rangle - \langle N_{am}\rangle\langle N_{am}\rangle} \quad (9)$$

where $R$ is the gas constant, $U_{ff}$ is the adsorbate–adsorbate potential energy, and $U_{fs}$ is the adsorbate–adsorbent potential energy. The adsorption selectivity of a mixture ($S$) at finite loading can be defined as

$$S = \frac{N_i}{\sum_{j,j\neq i} N_j} \times \frac{\sum_{j,j\neq i} p_j}{p_i} \quad (10)$$

All of the simulations are carried out using the RASPA 2.0 package.[31] The percent of gas adsorption (ER (%)) and selectivity ($ER_1$ (%)) without considering the partial charges of water are given by eqn (11a) and (11b).

$$ER(\%) = \frac{N_{without}}{N} \times 100\% \quad (11a)$$

$$ER_1(\%) = \frac{S_{without}}{S} \times 100\% \quad (11b)$$

where $N$ and $S$ are the gas adsorption amount and selectively in the dry 5A zeolite, respectively, and $N_{without}$ and $S_{without}$ are the gas adsorption amount and selectively in the wet 5A zeolite without considering the partial charges of water molecule, respectively.

# 3. Results and discussion

## 3.1. Model validation

To validate the accuracy of the force field parameters characterizing the interactions between $CO_2$, $N_2$, water vapor, and the 5A zeolite particle, the adsorption isotherms of $CO_2$, $N_2$, and water vapor are simulated and compared to the experimental data. Fig. 2(a) shows the simulation results for the adsorption isotherms of $CO_2$ and $N_2$ in the 5A zeolite particle for the pressures ranging from 0 kPa to 100 kPa at 273 K and 295 K, respectively. The corresponding experimental data are also shown in Fig. 2(a) for comparison.[18,32] The relative deviations of the simulation results from the experimental data for $N_2$ and $CO_2$ gas adsorption are 1.6–30% and 7.5–36.0%, respectively. It is difficult to remove the $CO_2$ and $N_2$ adsorbed in 5A zeolites, so that the experimental values are lower than the values obtained by the simulations. Fig. 2(b) shows the simulation results for the adsorption isotherms of the water vapor adsorbed in the 5A

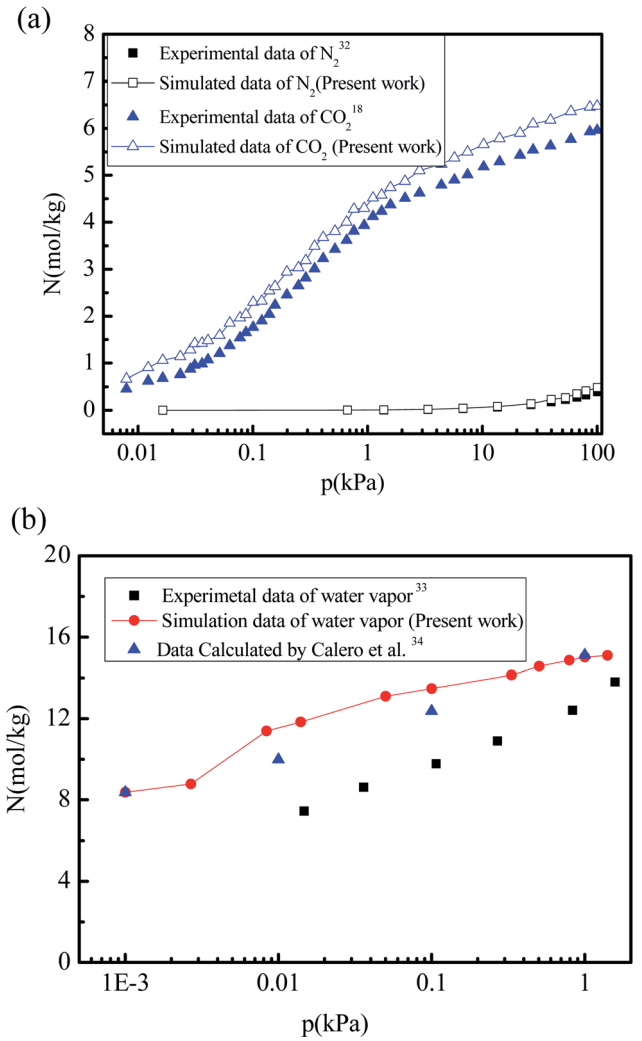


Fig. 2 Comparison of the simulation results with experimental data and with the simulation results reported in the literature. (a) Adsorption isotherms of $CO_2$ and $N_2$ adsorbed in 5A zeolite. (b) Adsorption isotherms of water vapor adsorbed in 5A zeolite.

zeolite at the pressures ranging from 0.003 kPa to 1.58 kPa at 298 K, compared to the experimental data[33] and to the simulation results obtained by Calero *et al.*[34] Similar to the results for $CO_2$ and $N_2$, it is very difficult to remove the water adsorbed in 5A zeolite, and this also leads to the lower experimental values compared to the simulation data. In order to verify the force filed parameters used in the present work, the present results are compared with the calculated data from Calero *et al.*[34] As can be seen from Fig. 2(b), the present results are consistent with the molecular simulation data reported by Calero *et al.*,[34] which indicates the reliability of the present work. To summarize, the proposed method accurately predicts the amounts of adsorbed $CO_2$, $N_2$ and $H_2O$ and thus can be used for further study.

### 3.2. Effect of water adsorption on the single gas adsorption

To understand the mechanism of the effect of the trace amount of water vapor on single gas adsorption, the $CO_2$, $N_2$, and water vapor adsorption amounts at different trace amounts of water vapor with and without considering the partial charges of water molecule are investigated.

Fig. 3 shows the $CO_2$ adsorption isotherm in 5A zeolite under different concentrations of water vapor (0, 0.05, 0.1, 0.3, 0.5, 1, 3, and 5 ppm) at pressures ranging from 0 to 120 kPa at 288 K. In all cases, the amount of adsorbed $CO_2$ first increases rapidly with increasing pressure (0–10 kPa), and then increases slowly to reach the saturation adsorption amount for the pressures in the 10–120 kPa range. Furthermore, as the water vapor concentration increases (0.3–5 ppm), the amount of adsorbed $CO_2$ decreases in the entire pressure range. This is due to the competitive adsorption effect for the $CO_2$ and $H_2O$ molecules. The $H_2O$ molecules have a negative effect on the $CO_2$ adsorption amount in 5A zeolite at a high concentrations of water vapor (>0.5 ppm), similar to that reported in X-type zeolites.[35,36] This demonstrates that a large fraction of the strong $CO_2$ adsorption sites will disappear due to the enhancement of the short-range Lennard-Jones repulsive interactions from the water molecules at high water vapor concentrations (>0.5 ppm). Surprisingly, for the water vapor concentrations being 0.1 ppm and 0.05 ppm, the amount of adsorbed $CO_2$ can be enhanced by 0.7–53.4% compared to that in the dry 5A zeolite in the entire pressure range; in particular, in the low pressure range (0–10 kPa), the enhancement is in the 3.0–53.4% range. This can be explained as follows. At a low water vapor concentration (<0.1 ppm), when the water molecules adsorb on the metal sites, their positions will be held relatively fixed due to the bonding of one of the water molecule's hydrogen atoms directed toward the metal center of the 5A zeolite structure, and due to the electronegative oxygen atom exposed and directed toward the center of the cavity in the 5A zeolite. This allows $CO_2$ to enter the center of the cavity with minimal steric repulsion and to interact favorably through electrostatic interactions with the adsorbed water molecules.[37] However, at high water vapor concentrations (>0.3 ppm), few $CO_2$ molecules can enter the cavity, and thus the amount of adsorbed $CO_2$ decreases.

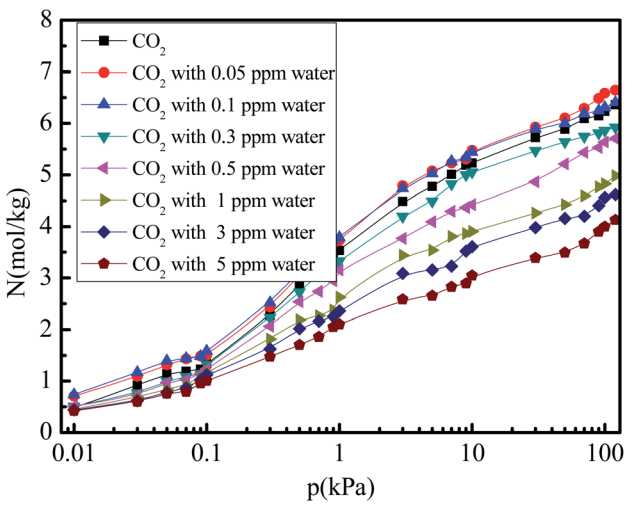


Fig. 3 Simulated $CO_2$ adsorption equilibrium isotherms in 5A zeolite under different amounts of trace water vapor.

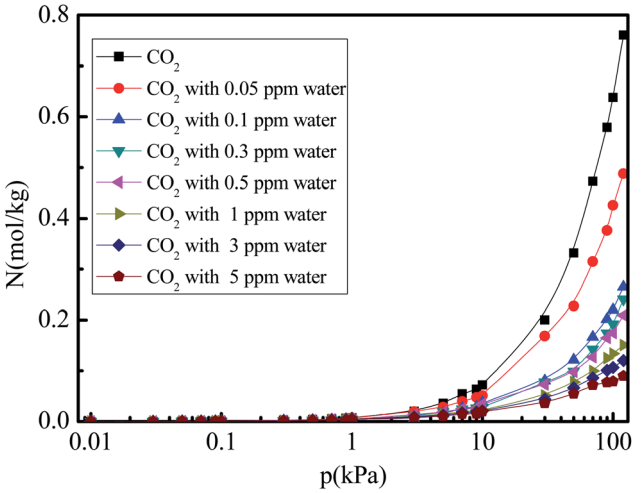


Fig. 4 Simulated $N_2$ adsorption equilibrium isotherm in 5A zeolite under different amounts of trace water vapor.

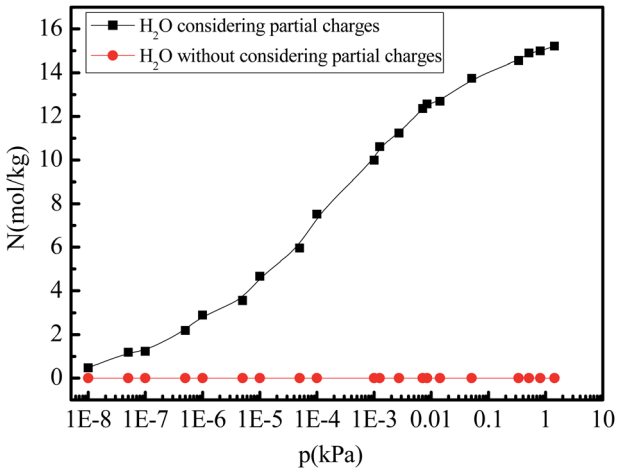


Fig. 5 Simulated $H_2O$ adsorption amounts at different pressures with the partial charge of water molecule switched on/off.

Fig. 4 shows the $N_2$ adsorption isotherm in 5A zeolite under different water vapor concentrations (0, 0.05, 0.1, 0.3, 0.5, 1, 3, and 5 ppm) for the pressures in the 0–120 kPa range at 288 K. In all cases, the amounts of adsorbed $N_2$ increase linearly in the entire pressure range. The $N_2$ adsorption amount decreases with increased water vapor concentration for all cases, implying the presence of competitive adsorption effect for the $N_2$ and water molecules. The water molecules occupy the adsorption sites of 5A zeolite. Moreover, the amount of adsorbed $CO_2$ is higher than that of adsorbed $N_2$, as observed from the comparison of Fig. 3 and 4, because the $CO_2$ molecule has a larger quadrupole moment and higher polarizability compared to the $N_2$ molecule as shown in Table 1. This means that the interactions between the $CO_2$ molecule and zeolite 5A are stronger than those for the $N_2$ molecules.

Given that the atomic partial charges of the adsorbate affect gas adsorption and separation,[8,38] we further investigate the role of the partial charges of the water molecule on the gas adsorption amount by switching them off during the simulations. Fig. 5 shows the pure water vapor adsorption amount varying with different pressures (0–1.0 kPa) at 288 K when the partial charges of water molecule are switched on and off. The amount of water vapor adsorption in 5A zeolite can increase to the saturation adsorption amount at the low pressure. It is also noted that the water vapor adsorption amount in 5A zeolite without considering the partial charges reduces to zero.

Table 1 Quadrupole moments and polarizability of $CO_2$ and $N_2$ molecules[35]

| Molecular properties | $CO_2$ | $N_2$ |
|---|---|---|
| Quadrupole ($cm^2$) | $-14.31 \pm 0.74 \times 10^{-40}$ | $-4.65 \pm 0.08 \times 10^{-40}$ |
| Polarizability ($cm^3$) | $2.91 \times 10^{-24}$ | $1.74 \times 10^{-24}$ |

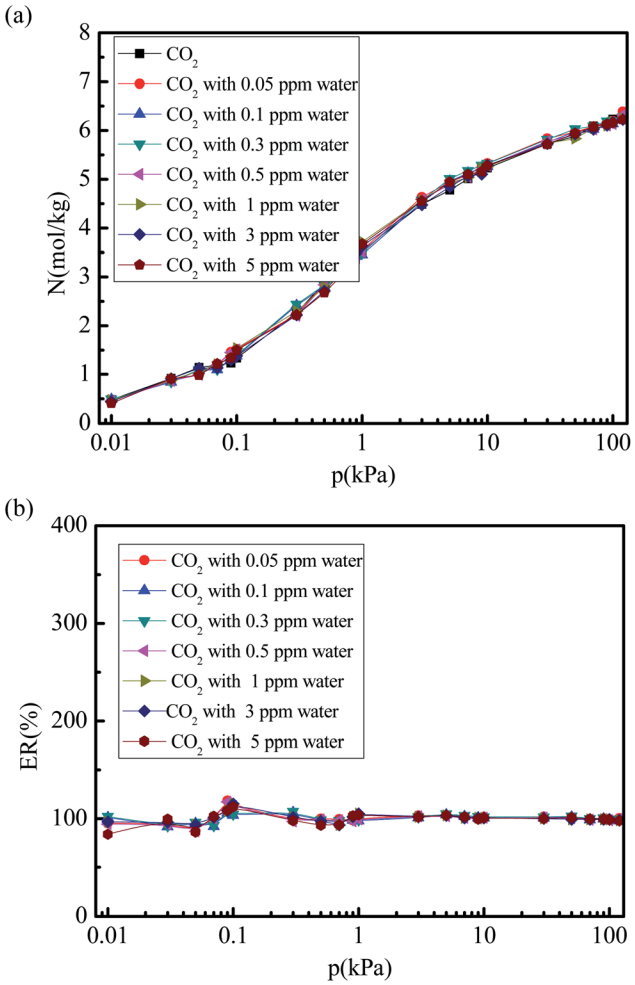


Fig. 6 Simulated $CO_2$ adsorption equilibrium isotherm and adsorption percent in 5A zeolite under different amounts of trace water vapor without considering the effect of the electrostatic interactions of water molecule. (a) $CO_2$ adsorption isotherm in 5A zeolite without considering the effect of the electrostatic interaction of molecule. (b) Percent of $CO_2$ adsorption amount without considering partial charges of water molecule.

Fig. 6 and 7 show the $CO_2$ and $N_2$ adsorption isotherms in 5A zeolite particle under different water vapor concentrations (0, 0.05, 0.1, 0.3, 0.5, 1, 3, and 5 ppm) at the pressures ranging from 0 kPa to 120 kPa at 288 K without considering the effect of the electrostatic interactions of water molecule. As shown in Figs. 6(a) and 7(a), when the partial charges of water molecule are switched off, the $CO_2$ and $N_2$ adsorption isotherms at different trace amounts of water vapor are similar to those in the dry 5A zeolite. The percent of $CO_2$ and $N_2$ without considering the partial charges of water molecule at the different concentrations of water vapor reaches ~100% and >50% compared to the amount of the adsorbed $CO_2$ and $N_2$ in the dry 5A zeolite as shown in Fig. 6(b) and 7(b), respectively. This illustrates that the partial charges of water molecule play a dominant role in influencing the $CO_2$ and $N_2$ adsorption amounts. To understand the mechanism of the effect of the trace amount of water vapor on the amounts of adsorbed $CO_2$ and $N_2$, the interactions between $CO_2$, $N_2$, water vapor, and 5A zeolite are investigated by calculating the adsorption heat of $CO_2$, $N_2$, and water vapor at infinite dilution condition, with the results shown in Table 2. The adsorption heat of water vapor in the present work is consistent with the experimental data ($100 \pm 25$ kJ mol$^{-1}$).[39] We note that the effects of the electrostatic interactions on the $CO_2$, $N_2$ and water vapor adsorption are obvious. That is, the electrostatic interactions between water and 5A zeolite are sufficiently strong to influence the $CO_2$ and $N_2$ adsorption performance.

Table 2 Adsorption heat at infinite dilution

| Adsorbate (kJ mol$^{-1}$) | $Q$ with adsorbate charges on | $Q$ with adsorbate charges off |
|---|---|---|
| $H_2O$ | 104.9 | 13 |
| $N_2$ | 22.5 | 12.5 |
| $CO_2$ | 56.4 | 36.4 |

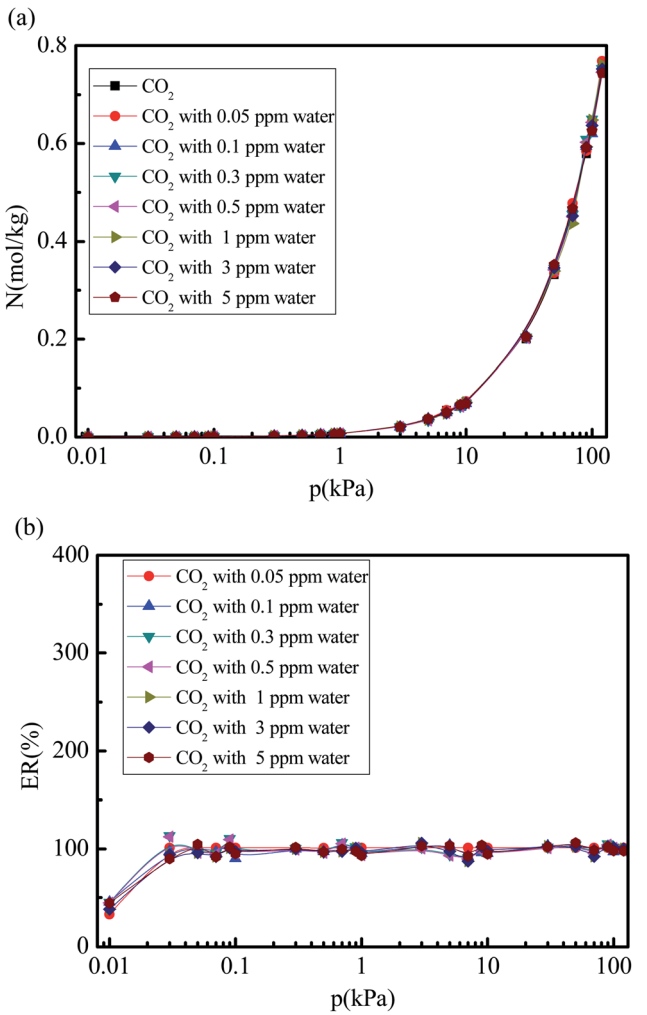


Fig. 7 Simulated $N_2$ adsorption equilibrium isotherm and adsorption percent in 5A zeolite under different amounts of trace water vapor without considering the effect of the electrostatic interactions of water. (a) $N_2$ adsorption isotherm in 5A zeolite without considering the effects of the electrostatic interactions of water molecule. (b) Fraction of the adsorbed $N_2$ amount without considering the partial charges of water molecule.

### 3.3. Effect of water vapor concentrations on the selectivity of the $CO_2/(N_2 + O_2)$ gas mixture

Gas mixture selectivity is important for practical applications of adsorption materials. Considering that the pressure for the low concentration $CO_2$ capture in space stations is approximately equal to the atmospheric pressure, the pressures in the 10–120 kPa range are adopted to study the selectivity of the $CO_2/(N_2 + O_2)$ gas mixture. Fig. 8 shows the selectivity of the $CO_2/(N_2 + O_2)$ gas mixture under different water vapor concentrations (0, 0.05, 0.1, 0.3, 0.5, 1, 3, and 5 ppm) at 288 K. The selectivity of the $CO_2/(N_2 + O_2)$ gas mixture decreases with increasing pressure under all water vapor concentrations. This trend is different from the operational conditions where $CO_2$ adsorption is below 0.1 ppm. This indicates the existence of a competitive adsorption effect between the $CO_2$ and $N_2$ molecules, and the increase in the $N_2$

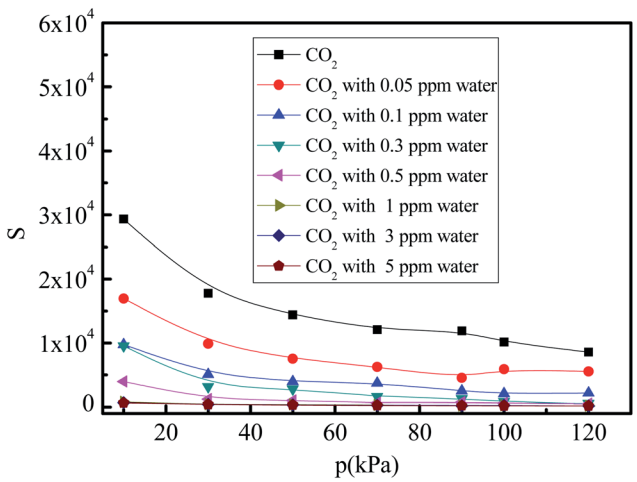


Fig. 8 Simulated $CO_2/(N_2 + O_2)$ gas mixture selectivity under different amounts of trace water vapor.

adsorption is more rapid than that for $CO_2$ adsorption in 5A zeolite, so that the strongly bound sites are occupied by the $N_2$ molecules before the weakly bound sites are filled with the $CO_2$ molecules. With an increase in the trace water amount, the selectivity of the $CO_2/(N_2 + O_2)$ gas mixture decreases in the entire pressure range. This can be explained as follows. The bond between the water and 5A zeolite is stronger than those for $N_2$ and $CO_2$, leadings to the $CO_2$ and $N_2$ adsorption shifting from the 5A zeolite framework structure to the α-cavity pore centers in 5A zeolite and to the exclusion of the $CO_2$ and $N_2$ molecules from the adjoining sites of sodium and calcium cations when water vapor is present in the $CO_2/(N_2 + O_2)$ gas mixture. At the high pressures (>30 kPa), since $H_2O$ clustering proceeds in different manner in 5A zeolite with sodium and calcium cations, the selectivity of the $CO_2/(N_2 + O_2)$ gas mixtures with the water vapor concentrations of greater than 0.3 ppm tends to zero.

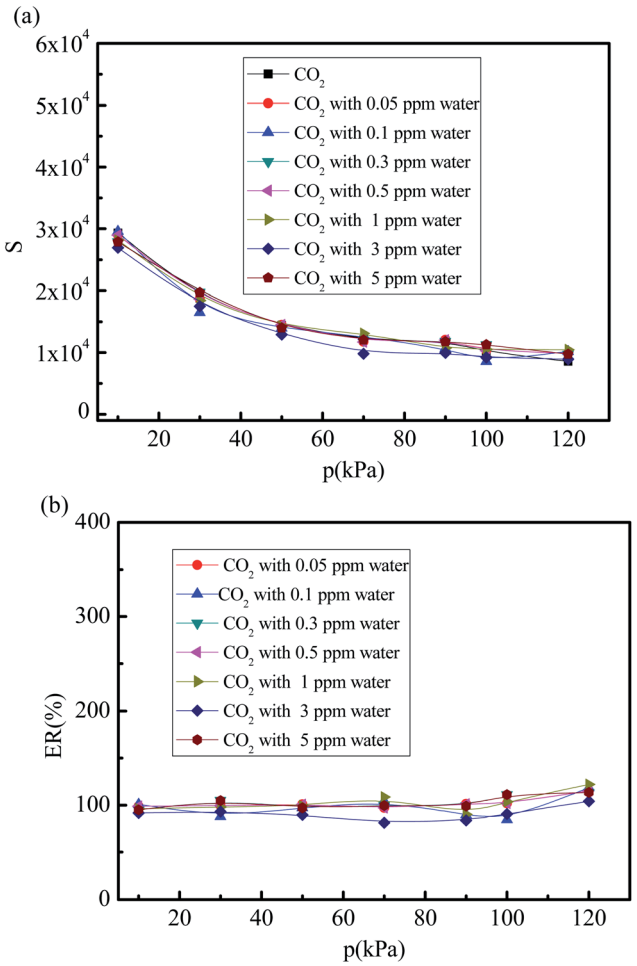


Fig. 9 Simulated $CO_2/(N_2 + O_2)$ gas mixture selectivity under different trace water vapor amounts without considering the effects of the electrostatic interactions of water molecule. (a) $CO_2/(N_2 + O_2)$ gas mixture selectivity without considering the effects of the electrostatic interactions of water molecule. (b) Percent of $CO_2/(N_2 + O_2)$ gas mixture selectivity without considering partial charges of water molecule.

Fig. 9(a) and (b) show the values and percent selectivity of the $CO_2/(N_2 + O_2)$ gas mixture under different water vapor concentrations (0, 0.05, 0.1, 0.3, 0.5, 1, 3, and 5 ppm) for the pressures in the 10–120 kPa range and temperature of 288 K without considering the effects of the electrostatic interactions of water molecule. As shown in Fig. 9(a), when the partial charges of water molecule are turned off, the selectivity of the $CO_2/(N_2 + O_2)$ gas mixture under different water vapor concentrations (0.05, 0.1, 0.3, 0.5, 1, 3, and 5 ppm) is similar to that in the dry 5A zeolite. The percent $CO_2/(N_2 + O_2)$ gas mixture selectivity without considering the partial charges of water molecule at different water vapor concentrations reaches over 80% compared with the selectivity in the dry 5A zeolite as shown in Fig. 9(b). This means that the substantial effects of water molecule are mainly attributed to the electrostatic interactions that are produced by the adsorbate due to the highly polar nature of the water molecules.

## 4. Conclusions

GCMC combining with DC-DFT simulation method is used to study the effects of the trace water vapor amounts on the low concentration $CO_2$ capture in 5A zeolite particles. The effects of a trace amount of water vapor on the amount of adsorbed $CO_2$ and $N_2$ are enhanced with increasing trace amount of water vapor due to the competitive adsorption between the $CO_2$, $N_2$ and water molecules. The amount of adsorbed $CO_2$ in 5A zeolite can be enhanced by 0.7–53.4% compared to that in the dry 5A zeolite with the mixture of below 0.1 ppm water vapor. Thus, a low concentration of water vapor (<0.1 ppm) is recommended for $CO_2$ adsorption in 5A zeolite. The amount of adsorbed $CO_2$ is higher than that of adsorbed $N_2$ adsorption because the $CO_2$ molecule has a large quadrupole moment and high polarizability. The percent of $CO_2$ and $N_2$ without considering the partial charges of water molecule at the different concentrations of water vapor reaches ~100% and >50% compared to the amount of the adsorbed $CO_2$ and $N_2$ in the dry 5A zeolite, respectively. The selectivity of the $CO_2/(N_2 + O_2)$ gas mixture decreases with increasing trace amount of water vapor because the partial charges of water molecule play the dominant role in the selectivity of the $CO_2/(N_2 + O_2)$ gas mixture. Thus, a lower water vapor concentration is recommended for the selectivity of the $CO_2/(N_2 + O_2)$ gas mixture in the 5A zeolite particle. The present work provides an in-depth understanding of the effects of a trace amount of water vapor on the low concentration $CO_2$ capture in space stations.

## Conflicts of interest

There are no conflicts to declare.

## Acknowledgements

This work was supported by the National Natural Science Foundation of China (No. 51806178), Natural Science Basic Research Plan in Shaanxi Province of China (No. 2019JQ-622) and the Fundamental Research Funds for the Central

Universities (No. G2018KY0303). We thank Dr H. J. Fang in David S. Sholl' group at Georgia Institute of Technology for the fruitful discussion on how to use the DC-DFT method to obtain the force field parameters among $CO_2$, water, and 5A zeolite.

## References

1 S. Satyapal, T. Filburn, J. Trela and J. Strange, Performance and properties of a solid amine sorbent for carbon dioxide removal in space life support applications, *Energy Fuels*, 2001, **15**, 250–255.

2 F. N. Ridha and P. A. Webley, Anomalous Henry's law behavior of nitrogen and carbon dioxide adsorption on alkali-exchanged chabazite zeolites, *Sep. Purif. Technol.*, 2009, **67**, 336–343.

3 D. Bahamon, A. Díaz-Márquez, P. Gamallo and L. F. Vega, Energetic evaluation of swing adsorption processes for $CO_2$ capture in selected MOFs and zeolites: effect of impurities, *Chem. Eng. J.*, 2018, **342**, 458–473.

4 K. N. Han, S. Bernardi, L. Z. Wang and D. J. Searles, Water diffusion in zeolite membranes: molecular dynamics studies on effects of water loading and thermostat, *J. Membr. Sci.*, 2015, **495**, 322–333.

5 M. Kraus, U. Trommler, F. Holzer, F. D. Kopinke and U. Roland, Competing adsorption of toluene and water on various zeolites, *Chem. Eng. J.*, 2018, **351**, 356–363.

6 B. S. Bal'zhinimaev, E. A. Paukshtis, A. V. Toktarev, E. V. Kovalyov, M. A. Yaranova, A. E. Smirnov and S. Stompel, Effect of water on toluene adsorption over high silica zeolites, *Microporous Mesoporous Mater.*, 2019, **277**, 70–77.

7 P. F. Zito, A. Brunetti, A. Caravella, E. Driolia and G. Barbieri, Water vapor permeation and its influence on gases through a zeolite-4A membrane, *J. Membr. Sci.*, 2019, **574**, 154–163.

8 H. Wang, L. Chen, Z. G. Qu, Y. Yin, Q. J. Kang, B. Yu and W. Q. Tao, Modeling of multi-scale transport phenomena in shale gas production — a critical review, *Appl. Energy*, 2020, 114575.

9 A. W. Thornton, D. A. Winkler, M. S. Liu, M. Haranczyk and D. F. Kennedy, Towards computational design of zeolite catalysts for $CO_2$ reduction, *RSC Adv.*, 2015, **5**, 44361.

10 O. Cheung and N. Hedin, Zeolites and related sorbents with narrow pores for $CO_2$ separation from flue gas, *RSC Adv.*, 2014, **4**, 14480.

11 H. Wang, Z. G. Qu, Y. Yin, J. Q. Bai and B. Yu, Review of molecular simulation method for gas adsorption/desorption and diffusion in shale matrix, *J. Therm. Sci.*, 2019, **28**(1), 1–16.

12 Y. Jing, L. Wei, Y. D. Wang and Y. X. Yu, Molecular simulation of MCM-41: structural properties and adsorption of $CO_2$, $N_2$ and flue gas, *Chem. Eng. J.*, 2013, **220**, 264–275.

13 H. Kim, W. Q. Deng, W. A. Goddard, S. S. Jang, M. E. Davis and Y. S. Yan, Sodium diffusion through aluminum-doped zeolite BEA system: effect of water solvation, *J. Phys. Chem. C*, 2009, **113**, 819–826.

14 W. Jeong and J. Kim, Understanding the mechanisms of $CO_2$ adsorption enhancement in pure silica zeolites under humid conditions, *J. Phys. Chem. C*, 2016, **120**, 23500–23510.

15 M. G. Ahunbay, Monte Carlo simulation of water adsorption in hydrophobic MFI zeolites with hydrophilic sites, *Langmuir*, 2011, **27**, 4986–4993.

16 L. Joos, J. A. Swisher and B. Smit, Molecular simulation study of the competitive adsorption of $H_2O$ and $CO_2$ in zeolite 13X, *Langmuir*, 2013, **29**, 15936–15942.

17 H. Wang, Z. G. Qu, J. Q. Bai and Y. S. Qiu, Combined grand canonical Monte Carlo and finite volume method simulation method for investigation of direct air capture of low concentration $CO_2$ by 5A zeolite adsorbent bed, *Int. J. Heat Mass Transfer*, 2018, **126**, 1219–1235.

18 H. Mohamdinejad, The adsorption of $CO_2/H_2O/N_2$ on 5A zeolite and silica gel in a packed column in one and two-dimensional flow, PhD thesis, University of Alabama in Huntsville, 1999.

19 M. Mofarahi and M. Seyyedi, Pure and binary adsorption isotherms of nitrogen and oxygen on zeolite 5A, *J. Chem. Eng. Data*, 2009, **54**, 916–921.

20 P. Gómez-Álvarez, J. Perez-Carbajo, S. R. G. Balestra and S. Calero, Impact of the nature of exchangeable cations on LTA-type zeolite hydration, *J. Phys. Chem. C*, 2016, **120**, 23254–23261.

21 S. Punnathanam, J. F. M. Denayer, I. Daems, G. V. Baron and R. Q. Snurr, Parallel tempering simulations of liquid-phase adsorption of n-alkane mixtures in zeolite LTA-5A, *J. Phys. Chem. C*, 2011, **115**, 762–769.

22 S. Calero and P. Gómez-Álvarez, Effect of the confinement and presence of cations on hydrogen bonding of water in LTA-type zeolite, *J. Phys. Chem. C*, 2014, **118**, 9056–9065.

23 H. J. Fang, A. Kulkarni, P. Kamakoti, R. Awati, P. I. Ravikovitch and D. S. Sholl, Identification of High-$CO_2$-capacity cationic zeolites by accurate computational screening, *Chem. Mater.*, 2016, **28**, 3887–3896.

24 A. García-Sánchez, C. O. Ania, J. Parra, D. Dubbeldam, T. J. H. Vlugt, R. Krishna and S. Calero, Transferable force field for carbon dioxide adsorption in zeolites, *J. Phys. Chem. C*, 2009, **113**, 8814–8820.

25 C. Guse and R. Hentschke, Simulation study of structural, transport, and thermodynamic properties of TIP4P/2005 water in single-walled carbon nanotubes, *J. Phys. Chem. B*, 2012, **116**(2), 751–762.

26 G. Kresse and J. Hafner, Ab-Initio molecular-dynamics simulation of the liquid-metal amorphous-semiconductor transition in germanium, *Phys. Rev. B: Condens. Matter Mater. Phys.*, 1994, **49**, 14251–14269.

27 G. Kresse and J. Furthmuller, Efficient iterative schemes for Ab Initio total-energy calculations using a plane-wave basis set, *Phys. Rev. B: Condens. Matter Mater. Phys.*, 1996, **54**, 11169–11186.

28 H. J. Fang, P. Kamakoti, P. I. Ravikovitch, M. Aronson, C. Paurb and D. S. Sholl, First principles derived, transferable force fields for $CO_2$ adsorption in Na-exchanged cationic zeolites, *Phys. Chem. Chem. Phys.*, 2013, **15**, 12882–12894.

 

29 H. J. Fang, H. Demir, P. Kamakoti and D. S. Sholl, Recent developments in first-principles force fields for molecules in nanoporous materials, *J. Mater. Chem. A*, 2014, **2**, 274–291.
30 H. J. Fang, P. Kamakoti, J. Zang, S. Cundy, C. Paur, P. I. Ravikovitch and D. S. Sholl, Prediction of $CO_2$ adsorption properties in zeolites using force fields derived from periodic dispersion-corrected DFT calculations, *J. Phys. Chem. C*, 2012, **116**, 10692–10701.
31 D. Dubbeldam, S. Calero, D. E. Ellis and R. Q. Snurr, RASPA: molecular simulation software for adsorption and diffusion in flexible nanoporous materials, *Mol. Simul.*, 2016, **42**, 81–101.
32 A. Martin-Calvo, J. B. Parra, C. O. Ania and S. Calero, Insights on the anomalous adsorption of carbon dioxide in LTA zeolites, *J. Phys. Chem. C*, 2014, **118**, 25460–25467.
33 Y. Wang and M. D. LeVan, Adsorption equilibrium of carbon dioxide and water vapor on zeolites 5A and 13X and silica gel: pure components, *J. Chem. Eng. Data*, 2009, **54**, 2839–2844.
34 S. Calero and P. Gómez-Álvarez, Effect of the confinement and presence of cations on hydrogen bonding of water in LTA-type zeolite, *J. Phys. Chem. C*, 2014, **118**, 9056–9065.
35 M. J. Purduea and Z. W. Qiao, Molecular simulation study of wet flue gas adsorption on zeolite 13X, *Microporous Mesoporous Mater.*, 2018, **261**, 181–197.
36 K. M. Lee, Y. H. Lim and Y. M. Jo, Evaluation of moisture effect on low-level $CO_2$ adsorption by ion-exchanged zeolite, *Environ. Technol.*, 2012, **33**, 77–84.
37 M. I. Hossain, J. D. Cunningham, T. M. Becker, B. E. Grabicka, K. S. Walton, B. D. Rabideau and T. G. Glover, Impact of MOF defects on the binary adsorption of $CO_2$ and water in UiO-66, *Chem. Eng. Sci.*, 2019, **203**, 346–357.
38 J. Y. Wu, Q. L. Liu, Y. Xiong, A. M. Zhu and Y. Chen, Molecular simulation of water/alcohol mixtures' adsorption and diffusion in zeolite 4A membranes, *J. Phys. Chem. B*, 2009, **113**, 4267–4274.
39 D. W. Breck, *Zeolite molecular sieves: structure, chemistry, and use responsibility*, Wiley, New York, 1974, pp. 83–90.